Inorg. Chem. **2006**, *45*, 8462–8464

Synthesis and Reactivity of a New Octanuclear Iron–Sulfur Nitrosyl Cluster

Harris Kalyvas and Dimitri Coucouvanis*

Department of Chemistry, University of Michigan, Ann Arbor, Michigan 48109

Received March 10, 2006

The synthesis and spectroscopic properties of $(PPN)_2[Fe_8S_6(NO)_8]$ as well as its reactivity toward sulfur are reported.

Nitric oxide (NO) plays a significant role in biology as a signaling molecule.[1−3] Various iron−sulfur nitrosyl clusters are known, and $(NH_4)[Fe_4S_3(NO)_7]$[4] (**1**), also known as the Roussin black salt, is the most well-studied member of this class. It is also recognized as an important physiological NO donor.[5−8]

The Roussin black salt is one of the few iron−sulfur clusters that possesses the sulfur-voided $[Fe_4S_3]$ cuboidal subunit found in the FeMo cofactor of nitrogenase[9] (Figure 1). Other clusters with structural subunits of similar topology include the $[MoFe_3S_3]$[10−12] and $[MFe_4S_6]$ (M = Mo, V)[13] clusters. In our investigations toward synthetic models for the nitrogenase clusters, we are exploring the reactivity of the Roussin black salt as a potential building block in the synthesis of clusters relevant to the FeMo cofactor of nitrogenase.

In this Communication, we report on the synthesis of the octanuclear iron−sulfur nitrosyl cluster $(PPN)_2[Fe_8S_6(NO)_8]$

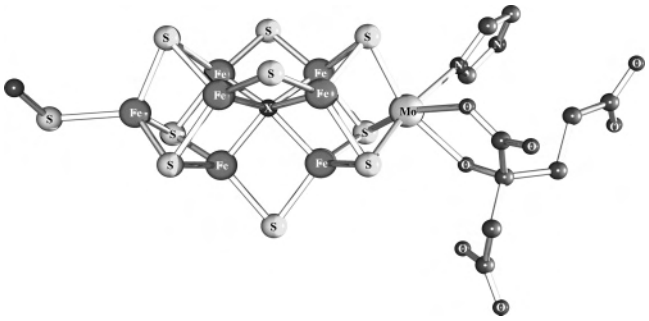

Figure 1. Structure of the FeMo cofactor of nitrogenase. The structure can be viewed as two M_4S_3 cuboidal units bridged by three μ_2-S atoms and a μ_6-X (X = C, N, or O) interstitial atom.

[**2**; PPN = bis(triphenylphospine)iminium] and its reactivity with sulfur. The reaction of **1** with $(PPN)_2[Fe_4(CO)_{13}]$ in a 2:3 ratio affords the new cluster **2** in high yield (90%). The other products of this reaction that were verified by IR and mass spectrometry (MS) are mainly $(PPN)[Fe(CO)_3(NO)]$ and a small amount of $(PPN)[Fe_4N(CO)_{12}]$. The reaction appears to proceed through the abstraction of nitrosyls from $[Fe_4S_3(NO)_7]^-$ by the $[Fe_4(CO)_{13}]^{2-}$ cluster and the possible formation of an $[Fe_4S_3(NO)_4]^-$ intermediate, which subsequently self-couples to form the $[Fe_8S_6(NO)_8]^{2-}$ cluster. $(PPN)[Fe(CO)_3(NO)]$ seems to be the main product formed by the reaction of the abstracted NO^+ with $[Fe_4(CO)_{13}]^{2-}$, while generation of the $[Fe_4N(CO)_{12}]^-$ cluster is not unexpected considering that the synthesis of this cluster occurs by the reaction of $Fe_3(CO)_9$ with $[Fe(CO)_3(NO)]^-$.[14,15]

The crystallographic structure determination of **2** (Figure 2) reveals a cubic arrangement of Fe atoms, with S atoms capping the faces of the cube. The cluster has average Fe−Fe and Fe−S distances of 2.66 and 2.26 Å, respectively. The nitrosyls are almost linearly bound to the Fe atoms with mean Fe−NO distances of 1.67 Å and Fe−N−O angles of 176.9°.

This cubic Fe_8S_6 type of arrangement is also known in the $(Et_4N)_3Fe_8S_6I_8$ (**3**),[16] $(PhCH_2NEt_3)_4Fe_8S_6I_8$ (**4a**), $[Fe(dppe)(MeCN)_4]_2Fe_8S_6I_8$ (**4b**),[17] and $Fe_8S_6(PCy_3)_4Cl_4$ (**5**)[18] clusters.

* To whom correspondence should be addressed. E-mail: dcouc@umich.edu.

(1) McCleverty, J. A. *Chem. Rev.* **2004**, *104* (2), 403−418.
(2) Butler, A. R.; Megson, I. L. *Chem. Rev.* **2002**, *102* (4), 1155−1165.
(3) Hayton, T. W.; Legzdins, P.; Sharp, W. B. *Chem. Rev.* **2002**, *102* (4), 935−991.
(4) Roussin, F. Z. *Ann. Chim. Phys.* **1858**, *52*, 285.
(5) Flitney, F. W.; Megson, I. L.; Butler, A. R. *J. Physiol. (Oxford, U.K.)* **1993**, *459*, P89−P89.
(6) Flitney, F. W.; Megson, I. L.; Thomson, J. L. M.; Kennovin, G. D. *J. Physiol. (Oxford, U.K.)* **1993**, *459*, P90−P90.
(7) Flitney, F. W.; Megson, I. L.; Thomson, J. L. M.; Kennovin, G. D.; Butler, A. R. *Brit. J. Pharmacol.* **1996**, *117* (7), 1549−1557.
(8) Flitney, F. W.; Megson, I. L.; Flitney, D. E.; Butler, A. R. *Brit. J. Pharmacol.* **1992**, *107* (3), 842−848.
(9) Einsle, O.; Tezcan, F. A.; Andrade, S. L. A.; Schmid, B.; Yoshida, M.; Howard, J. B.; Rees, D. C. *Science* **2002**, *297* (5587), 1696−1700.
(10) Tyson, M. A.; Coucouvanis, D. *Inorg. Chem.* **1997**, *36* (18), 3808−3809.
(11) Coucouvanis, D.; Han, J. H.; Moon, N. *J. Am. Chem. Soc.* **2002**, *124* (2), 216−224.
(12) Han, J. H.; Beck, K.; Ockwig, N.; Coucouvanis, D. *J. Am. Chem. Soc.* **1999**, *121* (44), 10448−10449.
(13) Cen, W.; Macdonnell, F. M.; Scott, M. J.; Holm, R. H. *Inorg. Chem.* **1994**, *33* (25), 5809−5818.
(14) Fjare, D. E.; Gladfelter, W. L. *Inorg. Chem.* **1981**, *20* (10), 3533−3539.
(15) Fjare, D. E.; Gladfelter, W. L. *J. Am. Chem. Soc.* **1981**, *103* (6), 1572−1574.

10.1021/ic060417r CCC: $33.50
Published on Web 09/15/2006

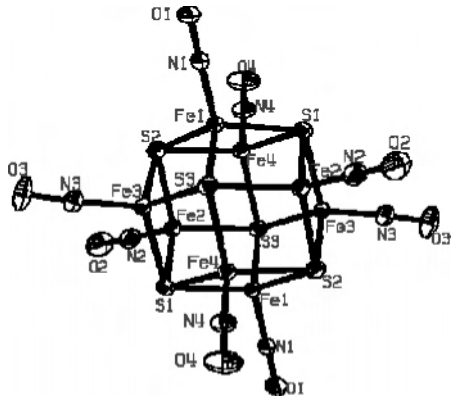

Figure 2. ORTEP diagram of $[Fe_8S_6(NO)_8]^{2-}$ showing thermal ellispoids with 50% probability.

Table 1. Comparison of the Average Distances between Different $Fe_8S_6X_8$ Clusters

	2	**3**[16]	**4a**[17]	**4b**[17]	**5**[18]
Fe−Fe	2.659	2.723	2.704	2.698	2.698
Fe−S	2.256	2.315	2.317	2.319	2.309
Fe−X	1.674	2.535	2.59	2.593	2.218 (Fe−Cl) 2.422 (Fe−PCy_3)

A comparison of distances in these clusters (Table 1) reveals a more compact structure for the $[Fe_8S_6(NO)_8]^{2-}$ cluster. On the basis of the linearity of the Fe−NO groups, one may adopt the $[NO]^+$ formalism to approximate the cluster oxidation levels.

The IR spectrum of **2** shows a NO stretch at 1684 cm^{-1}, which is within the range of NO^+. Negative MS shows a peak at *m*/*z* 878.6 that corresponds to $[Fe_8S_6(NO)_8]^-$ and several fragments of this molecule.[19] Magnetic susceptibility measurements give μ_{eff} of 0.79 (2 K), 1.04 (5 K), and 4.14 (300 K).

Cyclic voltammetry of **2** in dimethylformamide (DMF) vs Ag/AgCl reference electrode shows four reversible reductions (Figure 3) with half-wave potentials of $E_{1(rev)} = -480$ mV, $E_{2(rev)} = -620$ mV, $E_{3(rev)} = -1200$ mV, and $E_{4(rev)} = -1300$ mV. The occurrence of two pairs of closely spaced waves in **2**, at present, is difficult to interpret, although it has been observed numerous times on very pure crystalline samples. In various solvents, the shape of the voltammogram remains constant using scan rates from 20 to 200 mV/s and temperatures between −40 and +80 °C.

Upon reduction of **2** using an excess of potassium anthracenide, the two-electron-reduced $[Fe_8S_6(NO)_8]^{4-}$ cluster has been isolated as both PPN^+ and K^+ salts, with the later being crystallographically characterized and identified as a $K_4(DMF)_{13}[Fe_8S_6(NO)_8]$ (**6**) cluster. The IR shows two NO stretches at 1738 and 1686 cm^{-1}, and MS shows the same peaks as **2** with the addition of K^+- and PPN^+-containing

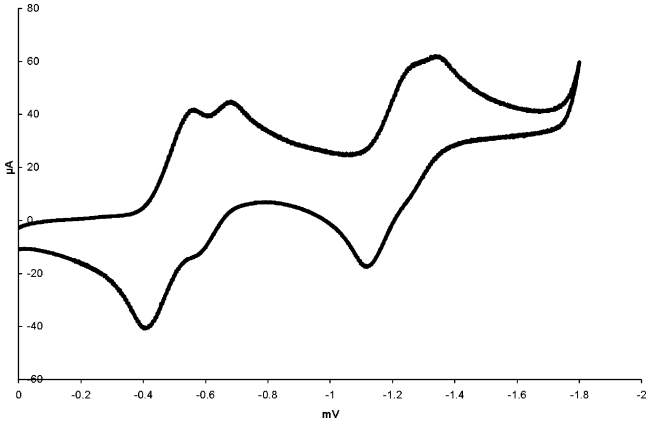

Figure 3. Cyclic voltammetry diagram of **2**.

Scheme 1. Schematic Representations of the Reactions of Iron Nitrosyl Clusters with Sulfur

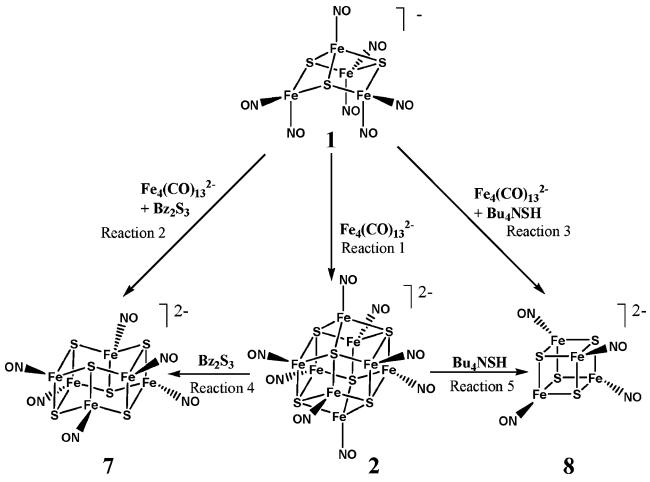

species. The structure of **6** is not significantly different from that of **2** and shows slightly smaller Fe−NO angles of the two nitrosyl ligands that appear to interact with the (DMF-coordinated) K ions. The cyclic voltammetry trace of the $(PPN)_4[Fe_8S_6(NO)_8]$ cluster is identical with that of **2** (Figure 3), providing further evidence that **2** remains intact during reduction.

Preliminary reactivity studies of cluster **2** have been explored using sulfur donor reagents in order to achieve clusters with different Fe/S ratios. The cluster $(PPN)_2[Fe_6S_6(NO)_6]$ [**7**; IR ν_{NO} 1679, 1669 cm^{-1}; ESI-MS *m*/*z* 707.3 ($[Fe_6S_6(NO)_6]^-$)] is formed by the reaction of benzyl trisulfide (Bz_2S_3) with **2** in a 3:1 molar ratio (reaction 4, Scheme 1). The reaction of **2** with tetrabutylammonium hydrogen sulfide (Bu_4NSH), in a 1:6 molar ratio, gives $(PPN)_2[Fe_4S_4(NO)_4]$ [**8**; reaction 5, Scheme 1; IR ν_{NO} 1652 cm^{-1}; ESI-MS *m*/*z* 471.5 ($[Fe_4S_4(NO)_4]^-$)]. The same products (**7** and **8**) are obtained when the corresponding sulfur reagents are introduced to the initial reaction of **1** with $(PPN)_2[Fe_4(CO)_{13}]$. With Bu_4NSH (reaction 3, Scheme 1), **8** is the only product, while in the case of Bz_2S_3 (reaction 2, Scheme 1), **7** is the main product, although smaller amounts of **8** are also formed. These conversions are shown in Scheme 1.

The yield of **7** (reaction 2, Scheme 1) is unreasonably high, assuming that $[Fe_4S_3(NO)_7]^-$ is the only source of iron in **7**.

(16) Pohl, S.; Saak, W. *Angew. Chem., Int. Ed. Engl.* **1984**, *23* (11), 907−908.
(17) Pohl, S.; Opitz, U. *Angew. Chem., Int. Ed. Engl.* **1993**, *32* (6), 863−864.
(18) Goh, C.; Segal, B. M.; Huang, J. S.; Long, J. R.; Holm, R. H. *J. Am. Chem. Soc.* **1996**, *118* (47), 11844−11853.
(19) It should be noted that, under the conditions used for our MS measurements, the observed peaks are always singly charged even for well-known iron−sulfur species such as $[Fe_4S_4Cl_4]^{2-}$.

Table 2. Electrochemical Comparison between the Reported Iron−Sulfur Nitrosyl Clusters and the PPN Analogues Reported in This Work

compound	obsd reduction potential (mV)			
$(PPN)_2[Fe_8S_6(NO)_8]$	−480	−620	−1200	−1300
$(PPN)_2[Fe_6S_6(NO)_6]$	−690		−1520	
$(Et_4N)_2[Fe_6S_6(NO)_6]$[21]	−730	−900	−1400	−1640
$(PPN)_2[Fe_4S_4(NO)_4]$	−200		−1280	
$Fe_4S_4(NO)_4$[22]	+130		−650	
$(PPN)[Fe_4S_3(NO)_7]$	−360		−1150	
$(Et_4N)[Fe_4S_3(NO)_7]$[20]	−680		−1260	

It appears therefore that the $[Fe_4(CO)_{13}]^{2-}$ cluster provides additional iron in the synthesis of **7**. In addition, it is known that $[Fe(CO)_3(NO)]^-$ upon reaction with sulfur(0) produces $[Fe_4S_4(NO)_4]^-$,[20] so the pathway of the formation of **7** through reaction 2 seems to be more complicated than the initial formation of **2** and further reaction with Bz_2S_3, as shown by reactions 1 and 4. The $[Fe_6S_6(NO)_6]^{2-}$ cluster has been synthesized previously[21] with different counterions but in lower yields. The crystal structure of **7** does not show any differences that could be attributed to effects from the counterion. The $[Fe_4S_4(NO)_4]^{2-}$ cluster has not been isolated in this oxidation level previously. The IR spectrum shows a NO stretch at 1652 cm^{-1}, which is lower compared to the 1760 and 1700 cm^{-1} reported for $Fe_4S_4(NO)_4$ and $[Fe_4S_4(NO)_4]^-$, respectively.[20] The lower frequency of the NO stretching vibration in **8** is consistent with the expected increase in the Fe−NO back-bonding in the dianionic **8**. Elemental analysis also is consistent with the $(PPN)_2[Fe_4S_4(NO)_4]$ formula; however, we were not able to obtain a satisfactory crystal structure because of the high distortion of the PPN cations in the crystal lattice. Nevertheless, the presence of an $Fe_4S_4(NO)_4$ cluster and two PPN cations was confirmed.

The electrochemistry of **7** under the same conditions as those in the case of **2** (DMF, Ag/AgCl) shows two reversible reductions at −690 and −1520 mV, while the reported cyclic voltammetry for $(Et_4N)[Fe_6S_6(NO)_6]$[21] shows four waves at −730, −900, −1400, and −1640 mV (Table 2). One possible reason for the appearance of two reductions instead of four is that the PPN^+ cation affects the spacing between the two consecutive one-electron reductions, causing them to overlap and exhibit a two-electron reduction wave.[22] A similar effect on the positions and spacing of the reduction potentials is also observed for **8**, which shows two reversible reductions at −200 and −1280 mV, as the reported $Fe_4S_4(NO)_4$ cluster[20] shows two waves at +130 and −650 mV. Finally, for $(PPN)[Fe_4S_3(NO)_7]$, two reversible waves are observed at −360 and −1150 mV, as opposed to −680 and −1260 mV reported in the literature for $(Et_4N)[Fe_4S_3(NO)_7]$.[23]

The reduction waves of **1** as a PPN salt and of **7** appear to be in close proximity to the reduction waves of **2**. Samples of **2** were "spiked" with **1** and **7** to explore the possibility that the latter may be impurities in **2**. The voltammetry trace of the "spiked" **2** showed the waves of **2** and additional reduction waves due to **1** and **7,** respectively. These results and the identical voltammetric trace shown by the two-electron-reduced derivative of **2** strongly indicate that the unusual cyclic voltammetry trace of **2** (Figure 3) is not due to a mixture of two species.

The **2** cluster is the first example of an octanuclear iron−sulfur nitrosyl cluster, and reactivity studies presented in this Communication indicate that iron−sulfur nitrosyl clusters exhibit similar transformations between tetra-, hexa-, and octanuclear clusters, as observed previously in the iodo-Fe_8S_6 clusters.[16,17]

Further investigations of the reactivities of these new octanuclear iron−sulfur clusters are presently underway.

Acknowledgment. We thank Dr. Jeff Kampf for X-ray data collection. The authors acknowledge the support of this work by a grant from the National Institutes of Health (Grant GM 33080).

Supporting Information Available: Detailed synthetic procedures and spectroscopic data of compounds **2**, **6**, **7**, and **8** and graphs of the cyclic voltammetry experiments discussed herein as well as X-ray crystallographic files in CIF format for **2**, **6**, and **7** are provided. This material is available free of charge via the Internet at http://pubs.acs.org.

IC060417R

(20) Chu, C. T. W.; Lo, F. Y. K.; Dahl, L. F. *J. Am. Chem. Soc.* **1982**, *104* (12), 3409−3422.
(21) Scott, M. J.; Holm, R. H. *Angew. Chem., Int. Ed. Engl.* **1993**, *32* (4), 564−566.
(22) Gosser, D. K. *Cyclic voltammetry: simulation and analysis of reaction mechanisms*; VCH: New York, 1993.
(23) Daddario, S.; Demartin, F.; Grossi, L.; Iapalucci, M. C.; Laschi, F.; Longoni, G.; Zanello, P. *Inorg. Chem.* **1993**, *32* (7), 1153−1160.

(24) All diffraction data were collected on a Bruker P4 X-ray diffractometer operated at 153 K ($2\theta_{max}$ = 56.57, 56.57, and 56.51° for **2**, **6**, and **7**, respectively). The space group $P\bar{1}$, triclinic, for all three structures was determined based on systematic absences and intensity statistics. Cell dimensions (Å, deg) for **2**: a = 10.8007(11), b = 14.6681(15), and c = 14.9851(15) with α = 117.4000(10), β = 97.671(2), γ = 96.071(2), and V = 2050.78 Å^3, Z = 1. Cell dimensions (Å, deg) for **6**: a = 12.121(5), b = 15.585(5), and c = 22.218(5) with α = 88.524(5), β = 85.215(5), γ = 68.150(5), and V = 3881.95 Å^3, Z = 2. Cell dimensions (Å, deg) for **7**: a = 13.0510(14), b = 13.3561(14), and c = 13.3741(14) with α = 118.473(2), β = 91.213(2), γ = 95.004(2), and V = 2036.2 Å^3, Z = 2. Full-matrix least-squares refinement based on F^2 converged to R1 [$I > 2\sigma$] values of 0.0314, 0.0562, and 0.0325 and wR2 values of 0.0877, 0.1788, and 0.0716, with GOF = 1.025, 1.030, and 1.022, for **2**, **6**, and **7**, respectively.